IEEE Access
Multidisciplinary | Rapid Review | Open Access Journal

Received January 26, 2022, accepted February 20, 2022, date of publication February 24, 2022, date of current version March 4, 2022.

Digital Object Identifier 10.1109/ACCESS.2022.3154064

On the Behavior of Self-Triplexing SIW Cavity Backed Antenna With Non-Linear Replicated Hybrid Slot for C and X-Band Applications

AMIT KUMAR[1], MUNISH KUMAR[2], (Graduate Student Member, IEEE), AND AMIT KUMAR SINGH[1]

[1]Department of Electronics Engineering, IIT BHU, Varanasi, Uttar Pradesh 221005, India
[2]University School of Information, Communication and Technology, Guru Gobind Singh Indraprastha University (GGSIPU), Dwarka, New Delhi 110078, India

Corresponding author: Amit Kumar (amitk.rs.ece17@iitbhu.ac.in)

ABSTRACT In this paper, a substrate integrated waveguide (SIW) based self-triplexing antenna (STA) with non-linear replicated hybrid slot (NLR-HS) is presented. To the author's best knowledge, the concept of NLR is the first of its kind in the literature used for obtaining self-triplexed operation. Initially, the SIW cavity is loaded by a hexagonal slot merged with two rectangular transverse slots that together produce two distinct resonances around 5.23 and 7.50 GHz. The variation in resonant frequencies of both lower and upper frequency bands can be modelled by applying NLR on the hexagonal slot. To achieve the self-triplexing operation, a coaxial probe-fed parasitic hexagonal patch is placed concentrically inside the hexagonal slot. The third resonance is centered around 10.82 GHz and can be modelled with the help of the gap between the hexagonal slot and parasitic patch.To validate the proposed idea, the design is fabricated and experimentally tested. Moreover, the antenna shows a front-to-back ratio (FTBR) better than 25 dB, average isolation of 43 dB and measured gain (efficiency) values of 7.33 (97.39%), 6.66 (95.82%), and 6.28 (97.83%) dBi at three resonances. Good agreement between the simulated and measured results makes the proposed STA a good candidate for practical applications.

INDEX TERMS 5G, cavity-backed antenna, non-linear replication (NLR), self-triplexing, sub-6 GHz, substrate integrated waveguide (SIW).

I. INTRODUCTION

The rapid growth in wireless communication systems has increased the demand of multiband/multi-standard antennas for various operations [1]. Various wireless applications such as mobile handheld devices [2] and RF front-end systems [3] require multiple transceivers to operate in different frequency bands. Hence, self-multiplexed antennas receive huge attention due to their simple and compact size with no requirement of decoupling network [4], better isolation between the excitation ports and ease of integration with the RF front-end components [5], [6].

Different self-diplexing/triplexing antennas (SDA/STA) have already been designed in the previous literature using techniques such as defected ground structures (DGS) [7], metamaterial [8], multilayered configuration [9], split ring resonators (SRRs) [10] and spiral defected resonators [11]. However, tuning of resonant frequency in these multiplexers is hard to achieve. Also, their integration with the planar circuits (especially multilayered multiplexers) is highly difficult and challenging task [12]. Also, when a single patch is excited using orthogonally placed feed lines, the isolation between the ports is hard to achieve (especially when $\frac{f_H}{f_L}$ approaches 2) [13]. One solution to these problems is implementation using substrate integrated waveguide (SIW) technique that exhibits attracting features such as low back-lobe radiation, improved isolation between/among the excitation ports and easy integration with planar circuits [14]–[16]. Most recently, SIW based STAs with intrinsically isolated input ports and independently tuned frequency bands are discussed in [17], [18]. In [17], a SIW based STA having two bow-tie shaped slots are etched on a SIW cavity is proposed. The position of the slots is varied to obtain the three distinct independently tuned frequency bands centred around 7.89/9.44/9.87 GHz. Another SIW based STA designed for 4.18/5.2/5.8 GHz frequency bands is discussed

The associate editor coordinating the review of this manuscript and approving it for publication was Pavlos I. Lazaridis.

in [19] where two different SIW cavities are formed, i.e., outer cavity with two transverse slots for 4.18/5.2 GHz and inner cavity with annular slot for 5.8 GHz frequency band. A similar concept with modified outer cavity is presented in [20]. The outer and inner cavities of the proposed STA supports 4.8/5.4 GHz and 3.5 GHz frequency bands, proving its suitability for 3.5/4.8/5.4 GHz WLAN, WiMAX and 5G wireless standards. The STA presented in [21] uses the innovative concept of hybrid SIW cavity resonator (combination of half-mode circular and rectangular SIW cavities) for the generation of 5.57/7.17/7.65 GHz frequency bands. The excitation ports are separated with the help of T-shaped slots. Another STA supporting 5.6/6.64/6.95 GHz with T-shaped slot etched in the metallic ground plane is discussed in [22]. Here, three shorted-vias are introduced for good isolation of better than 25 dB among the excitation ports. Reference [23] also uses the idea of half-mode rectangular SIW cavity for 4.95/5.3/5.9 GHz WLAN wireless application. The proposed STA consists of an inverted V-shaped slot etched on the SIW cavity which divides it into two sub-cavities, one eight-mode while other one quarter-mode. Another STA with improved port isolation, i.e., more than 28.4 dB is proposed in [24]. The proposed STA comprises of modified I-shape slot intently designed for 4.14/6.1/8.32 GHz frequency bands. In [18], the reported work shows a dumbbell shaped slot placed on the SIW cavity to radiate at 6.76/8.62/13.33 GHz, thus supporting C-, X- and K_u frequency bands simultaneously. Though the aforementioned STAs achieve good performance characteristics such as high isolation among the excitation ports and gain/efficiency levels, still more compact and independently tuned STAs with lesser number of tuning parameters are needed to be explored.

Here, a compact SIW based STA with two orthogonally placed microstrip feed lines and one coaxial probe is presented. The proposed design consists of a single large SIW cavity designed over a single substrate layer with a hybrid slot which is a combination of a hexagonal slot and two narrow rectangular slots. After applying scaling non-linear replications (NLR) over the hexagonal slot in both vertical and horizontal directions, the self-diplexing operation with two resonances around 5.23 and 7.50 GHz is reported. For self-triplexing operation, the space inside the hexagonal slot is filled with similar parasitic hexagonal patch and fed by coaxial probe. This generates resonance around 10.82 GHz which can be modelled using the gap between the parasitic patch and hexagonal slot. The independent tuning of each frequency band, isolation and radiation characteristics are also discussed in detail. Finally, the proposed STA is fabricated using standard PCB process and good agreement between the experimental and simulated results is found. The main contributions of the proposed SIW based STA are:

1) To the author's best knowledge, the proposed SIW-based STA is the first of its kind in the literature where the concept of NLR is utilized for obtaining self-triplexed operation.

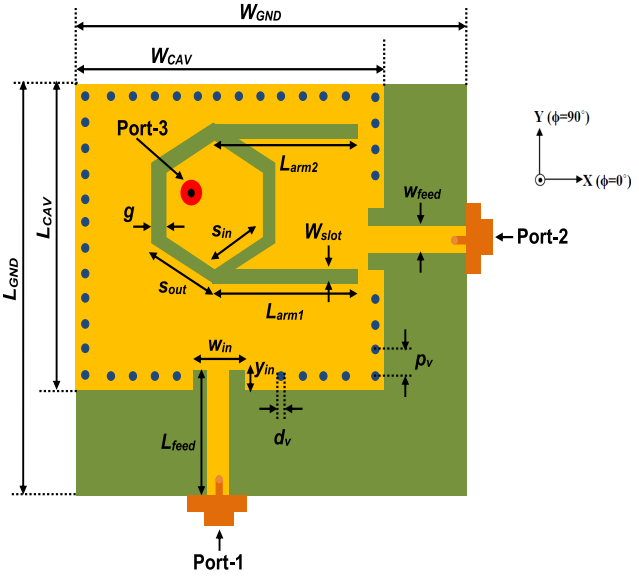

FIGURE 1. Schematic of the proposed antenna. The modal parameters are: $W_{GND} = 29$, $L_{GND} = 29$, $W_{CAV} = 24$, $L_{CAV} = 24$, $L_{arm1} = 9.5$, $L_{arm2} = 9.5$, $w_{slot} = 1.5$, $S_{in} = 5.5$, $S_{out} = 6$, g=0.5, $w_{feed} = 2$, $L_{feed} = 7.4$, $w_{in} = 2.4$, $y_{in} = 2.4$, $p_V = 2$ and $d_V = 1$ (Units: mm).

2) Easy independent tuning of all the three frequency bands is allowed using scaling of the hexagonal slot in x- and y-directions and spacing (or gap) between the hexagonal parasitic patch and hexagonal slot. Hence, the flexible operation of the proposed STA can be easily utilized for different frequency bands in C-, and X-band.
3) The proposed STA is highly compact as compared to already proposed SIW based STAs in the literature [17], [18] which added merit to the proposed design.
4) The orthogonal placement of the feed lines results into the weak coupling between the excitation ports, i.e., better than 43 dB. Therefore, the proposed antenna possesses the highest isolation as compared to existing STAs discussed in [17], [18].

II. PROPOSED ANTENNA DESIGN AND ANALYSIS

Fig. 1 illustrates the proposed SIW-based cavity-backed STA with finely tuned dimensions. The proposed STA design consists of a square SIW-cavity ($W_{CAV} \times L_{CAV}$), a regular hexagonal slot (side length, S_{out}) merged with two rectangular slots (slot-1: $w_{slot} \times L_{arm1}$, slot-2: $w_{slot} \times L_{arm2}$) and orthogonally placed feed lines, each having dimensions of $L_{feed} \times w_{feed}$. The proposed STA uses a 0.787 mm thick RT/Duroid-5880 with a dielectric constant $\varepsilon_r = 2.2$ and a dielectric loss tangent $\tan\delta = 0.0002$.

A. CAVITY DESIGN

The SIW cavity is implemented by scooping out the cylindrical vias of diameter d_V and pitch p_V from the substrate material used and filled them with the copper. Four rows of

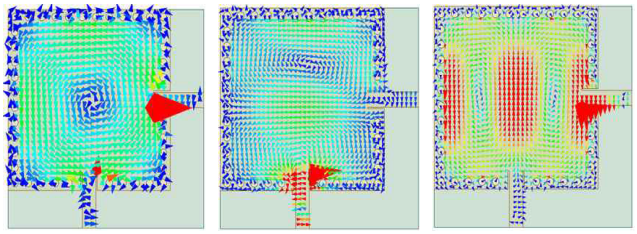

FIGURE 2. Vector H-field distribution of SIW cavity without any slot at (a) 6.88 GHz when only port-1 is ON (TE_{110}), (b) 10.89 GHz when only port-1 is ON (TE_{120}) and (c) 10.89 GHz when only port-2 is ON (TE_{210}).

such metal filled vias around the metallic patch make four sidewalls of the SIW cavity. The value of parameters d_V and p_V are chosen maintaining the condition $\frac{d_V}{\lambda_0} \leq 0.1$ and $\frac{d_V}{p_V} \geq 0.5$ (where λ_o is the free space wavelength) so as to ensure the negligible power leakage through the SIW cavity sidewalls [25]. The relationship between the resonating frequency of the SIW cavity with its dimensions is given as follows [26]

$$f_{mnp} = \frac{1}{2\sqrt{\varepsilon\mu}}\sqrt{(\frac{m}{W_{cav,eff}})^2 + (\frac{n}{L_{cav,eff}})^2 + (\frac{p}{c})^2} \quad (1a)$$

where

$$L_{cav,eff} = L_{cav} - 1.08\frac{d_V^2}{p_V} + 0.1\frac{d_V^2}{L_{cav}} \quad (1b)$$

$$W_{cav,eff} = W_{cav} - 1.08\frac{d_V^2}{p_V} + 0.1\frac{d_V^2}{W_{cav}} \quad (1c)$$

where ε and μ are the permittivity and permeability of the dielectric material used whereas m, n and p are the integers (=1, 2, 3,…) and denote the number of variations in the standing wave pattern corresponding to x-, y- and z-axis directions. For a square SIW cavity, i.e., $L_{cav,eff}=W_{cav,eff}$ and $m\neq n$, several orthogonal degenerate modes will start propagating inside the SIW cavity as shown in Fig. 2. When the square SIW cavity is fed with port-1 only (port-2 is terminated by 50Ω matched load), the TE_{110} and TE_{120} modes are excited at 6.88 GHz and 10.89 GHz as shown in Fig. 2(a) and 2(b), respectively. Similarly, the TE_{210} mode at 10.89 GHz as shown in Fig. 2(c) is excited inside the same cavity when fed from port-2 only (port-1 is terminated by 50Ω load).

B. SELF-DIPLEXING OPERATION

The hexagonal slot along with the two rectangular slots are not etched exactly at the center of the SIW cavity, i.e., the asymmetric placement of the hybrid-slot divides the whole SIW cavity into two fictitious asymmetric SIW cavities. As a result, two distinct frequency bands centered around 5.23 GHz and 7.50 GHz start resonating inside the SIW cavity when excited individually. Due to loading of the hybrid slot, the original TE_{110} and TE_{210} resonant modes get perturbed

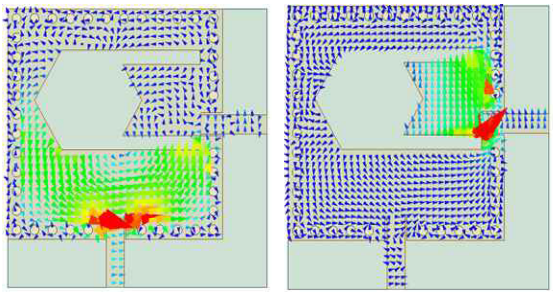

FIGURE 3. Vector H-field distribution with hybrid slot at (a) 7.50 GHz when only port-1 is ON (TE_{210}) and (b) 5.23 GHz when only port-2 is ON (TE_{110}).

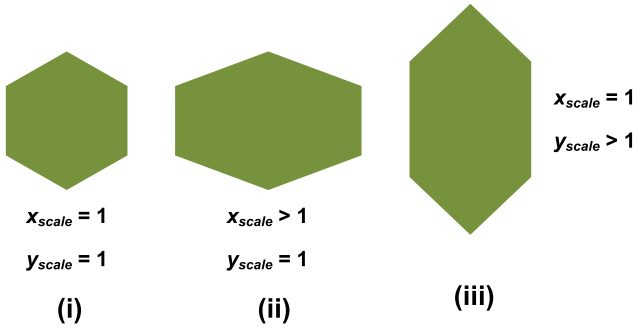

FIGURE 4. Hexagonal slot showing scaling as NLR in (i) no direction, (ii) x-direction only and (iii) y-direction only.

and new cavity modes with lower resonant frequency, i.e., at 5.23 and 7.50 GHz are generated. The vector H-field distribution at 5.23 GHz and 7.50 GHz resonating modes are illustrated in Fig. 3(a) and 3(b), respectively. A different current paths are created by TE_{210}/TE_{120} and TE_{110} modes propagating inside SIW cavity due to field concentration near port-1 and port-2, respectively. This results into creation of single transmission zero (TZ) around 7 GHz (as depicted by a dip in the isolation graphs discussed in next sub-sections) which lies between the two resonances, i.e., 5.23 and 7.50 GHz.

C. EFFECT OF NLR AND FREQUENCY TUNABILITY

The concept of NLR was first discussed in [27] where three different NLRs, i.e., elongation, cutting and distortion (or re-grouping) were discussed for obtaining desired flexibility in the radiation pattern of fractal antennas. Reference [28] utilizes elongation NLR on Sierpinski Knopp wide-slot structure for tri-band operation. On similar lines, elongation NLR is applied on the hexagonal slot and its effect of lower and upper resonant frequency is studied. Fig. 4 illustrates a basic NLR steps in a regular hexagon where scaling in x- and y-directions is regulated by two parameters, namely x_{scale} and y_{scale}, respectively. When there is no scaling in any direction, both x_{scale} and y_{scale} takes value equals to 1. With (x_{scale} >1, y_{scale}=1) and (y_{scale} >1, x_{scale}=1), there will be scaling in x- and y-directions, respectively.

The operating frequency of the proposed SDA with hybrid slot can be tuned independently by just varying the scaling parameters, i.e., x_{scale} and y_{scale} which makes the design more flexible for SDA operation. Fig. 5(a) illustrates the tuning of

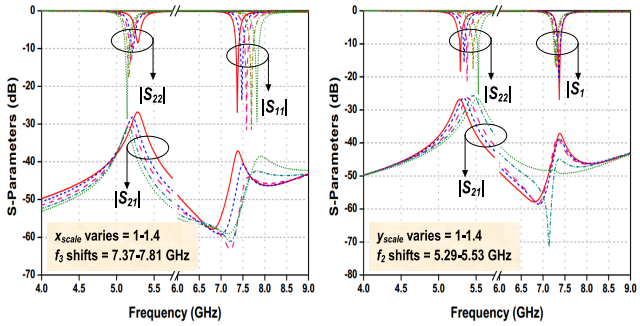

FIGURE 5. Independent frequency reform at (a) port-1 and (b) port-2 with x_{scale} (keeping y_{scale} constant, equals to 1) and y_{scale} (keeping x_{scale} constant, equals to 1), respectively. Shift in resonating frequency corresponding to parameter are noted in each figure.

7.50 GHz frequency band when x_{scale} is varied from 1.0 to 1.4 keeping y_{scale}=1. With $1.0 \leq x_{scale} \leq 1.4$, the resonating second operating frequency is shifted from 7.37 to 7.81 GHz due to decrease in capacitive loading while no significant variation in first operating frequency is noticed. Also, the isolation between the two ports gets from average 44.71 to 50.02 dB with variation in x_{scale} from 1.0 to 1.4, respectively.

Similarly, when y_{scale} is varied from 1.0 to 1.4, the first operating frequency changes from 5.29 to 5.53 GHz due to decrease in capacitive loading with minimal change in second operating frequency as shown in Fig. 5(b). The average isolation with $1.0 \leq y_{scale} \leq 1.4$ goes from 44.71 to 49.36 dB.

D. SELF-TRIPLEXING OPERATION

To obtain the self-triplexing operation, a parasitic hexagonal patch (similar to hexagonal slot) is placed concentrically inside the hexagonal slot. This parasitic hexagonal patch is excited by coaxial probe. Due to this configuration, the antenna now able to radiate at three different frequencies. The variation in the gap between the hexagonal patch and similar parasitic patch (or g) changes the coupling capacitance between them through dielectric region (C_{gd}) and through air (C_{ga}) that in turn changes the third resonating frequency around 10.82 GHz. The expressions for coupling capacitances C_{gd} and C_{ga} can be given by [29]

$$C_{gd} = (\frac{\varepsilon_r \varepsilon_0}{\pi}) ln\{coth(\frac{\pi g}{4h})\} + 0.65C_f[\frac{0.02}{g/h}\sqrt{\varepsilon_r} + 1 - \frac{1}{\varepsilon_r^2}] \tag{2a}$$

$$C_{ga} = \frac{1}{2}\varepsilon_0 \frac{K(k')}{K(k)} \tag{2b}$$

where $k = \frac{g}{g+2w}$, $k' = \sqrt{1-k^2}$ and

$$\frac{K(k')}{K(k)} = \begin{cases} \frac{1}{\pi} ln(2\frac{1+\sqrt{k'}}{1-\sqrt{k'}}) & 0 \leq k \leq 0.5 \\ \frac{\pi}{ln[2(\frac{1+\sqrt{k}}{1-\sqrt{k}})]} & 0.5 \leq k \leq 1 \end{cases} \tag{3}$$

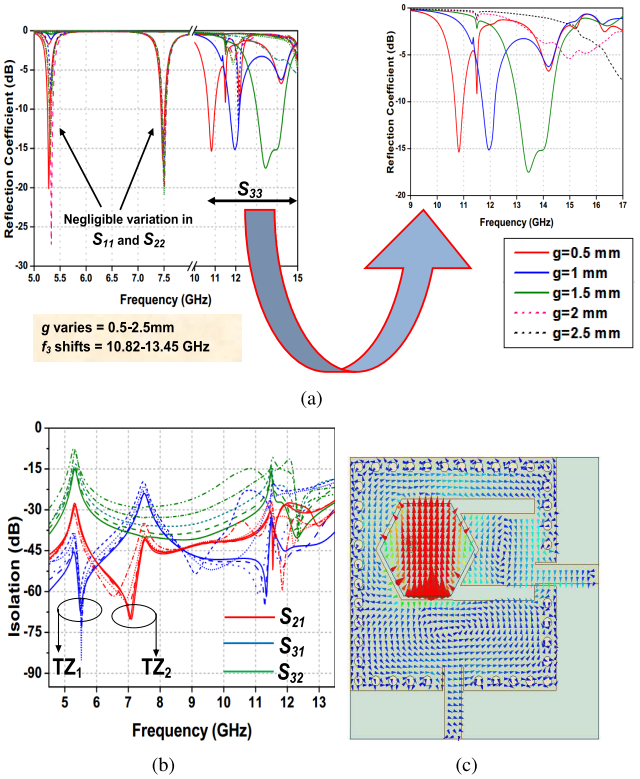

FIGURE 6. Tuning of third resonating frequency with varying values of g.

The independent tuning of the third operating frequency (f_{r3}) can be explicated by varying the parameter g. The change in g from 0.5 mm to 2.5 mm brings corresponding shift in f_{r3} from 10.82 GHz to 13.45 GHz due to increase in coupling capacitances as illustrated in Fig. 6(a). The port-3 exciting the parasitic hexagonal patch is placed asymmetric to both port-1 and port-2 which creates two TZs (TZ-1 in $|S_{31}|$ and TZ-2 in $|S_{21}|$) which improves the isolation of both port-1 and port-2 with port-3 (see Fig. 6(b)). The vector H-field distribution when the proposed STA is excited with port-3 only (keeping other ports terminated with 50Ω matched load) is shown in Fig. 6(c). It is seen that the proposed STA shows TE_{110} at 10.7 GHz with maximum intensity at the parasitic hexagonal patch only. In short, the features of the proposed STA can be concluded as following:

1) It operates at three different frequencies, i.e., f_{r1}=5.23 GHz, f_{r2}=7.50 GHz and f_{r3}=10.82 GHz. Independent tuning of the resonating frequencies is also possible.
2) Two TZs, one near 5.5 GHz in $|S_{31}|$ and other near 7 GHz in $|S_{21}|$ are generated due to orthogonal placement of the port-1 and port-2.
3) High isolation (>40 dB) among all the three ports is achieved due to their asymmetric and orthogonal placement with respect to each other.

The graphs showing shift in resonant frequency and their ratio(s) against parameters x_{scale}, y_{scale} and g affecting resonating frequencies f_{r1}, f_{r2} and f_{r3}, respectively are plotted

TABLE 1. Tunable ranges of operating frequencies and supporting applications.

Parameter Range	Frequency Range (GHz)	Supporting Applications
$1.0 \leq x_{scale} \leq 1.4$	$7.38 \leq f_{r1} \leq 7.81$ (Port-1)	LTE/LTE-Advanced, WLAN, and metrological satellite for weather monitoring
$1.0 \leq y_{scale} \leq 1.4$	$5.29 \leq f_{r2} \leq 5.53$ (Port-2)	WLAN and Wi-Fi
$0.5 \leq g \leq 2.5$	$10.82 \leq f_{r2} \leq 13.45$ (Port-3)	Amateur radio and amateur satellite operations

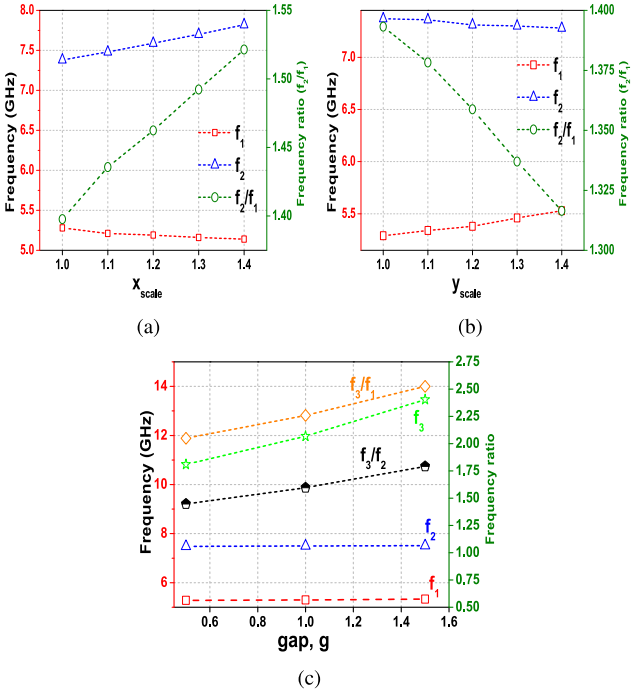

FIGURE 7. Variation in resonating frequencies f_{r1}, f_{r2} and f_{r3} against parameters (a) x_{scale}, (b) y_{scale} and (c) gap, g, respectively.

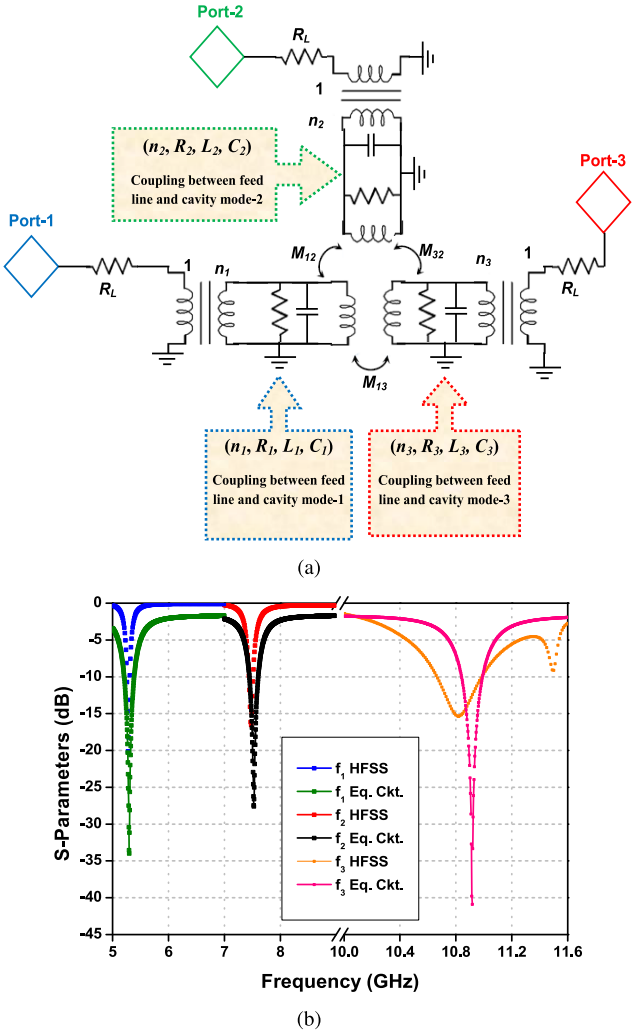

FIGURE 8. Independent frequency reform at (a) port-1 and (b) port-2 with x_{scale} (keeping y_{scale} constant, equals to 1) and y_{scale} (keeping x_{scale} constant, equals to 1), respectively. Shift in resonating frequency corresponding to parameter are noted in each figure. The modal parameters are: $n_1 = 3.18$, R_1=478Ω, $L_1 = 0.629$ nH, $C_1 = 1.4349$ pF, $n_2 = 6.172$, R_2=1.89 KΩ, $L_2 = 1.08$ nH, $C_2 = 0.414$ pF, $n_3 = 8.37$, $R_3 = 3.13$ KΩ, $L_3 = 0.793$ nH, $C_3 = 0.293$ pF.

in Fig. 7. This indicates that the each frequency ratios can be adjusted over a certain region as per the requirement.

E. EQUIVALENT CIRCUIT MODEL

Fig. 8(a) portrays the equivalent circuit of the SIW based STA, where each cavity mode is modelled as a parallel combination of R, L and C elements. The coupling between the feed and cavity can be modelled as a transformer with a shunt reactance and turns-ratio 1:n. The Circuit Design component of the ANSYS Electronics Desktop software (ver. 17.2) was used for optimizing the equivalent circuit model. The return loss (S_{11}) of the equivalent circuit model at each resonating frequency is compared with the equivalent circuit model in Fig. 8(b).

III. EXPERIMENTAL VALIDATION

In order to support the idea of SIW-based triple-band STA, a prototype of the proposed antenna is fabricated as shown in Fig. 9(a) and 9(b). The fabricated STA is characterized for validation and tested experimentally as shown in Fig. 9(c) and 9(d). Three low loss connectors are connected and soldered at three excitation ports and the measurement related to return losses (S_{11}/S_{22}/S_{33}) and isolation (S_{21}/S_{31}/S_{32}) is performed using Vector Network Analyzer (Agilent Technologies N5247A). The simulated and measured coefficients at all three ports are shown in Fig. 10(a). When excited with port-1, port-2 and port-3 individually (keeping other two ports terminated with 50Ω matched load), the measured (simulated) resonating frequencies f_{r1}, f_{r2}, and f_{r3} are 5.33 GHz (5.23 GHz), 7.53 GHz (7.50 GHz), and 11.02 GHz (10.82GHz) which are in acceptable limits. The isolation between the excitation ports, i.e., S_{21}, S_{31}, and S_{32} are also measured which are also found in good agreement with the simulated ones as illustrated in Fig. 10(b).

TABLE 2. Performance comparison with existing SIW-based STAs.

Reference	Physical Size (mm^2)	Electrical Size	Resonant frequency (GHz)	Isolation (dB)	Gain (dBi)	FTBR (dB)	Slot shape
[17]	23×32	$0.5\lambda_o^2$	7.89/9.44/9.87	22.5	7.2	17.3	Bow-tie
[19]	60×44	$1.08\lambda_o^2$	4.18/5.2/5.8	42/23.7/22.5	6.56/4.2/5.85	19	One annular slot and two transverse slots
[20]	-	$0.69\lambda_o^2$	3.5/4.8/5.4	26	4.5/5.9/6	16.1/18.5/22.8	One annular slot and two transverse slots
[21]	34.5×29.10	$0.42\lambda_o^2$	6.53/7.65/9.09	19	3.1/4.7/3.9	13.2	T-shape
[22]	48×48		5.6/6.64/6.95	23.8	-	-	T-shape
[23]	12.6×26.9	$0.08\lambda_o^2$	4.95/5.3/5.9	20.5	4.5/4.9/6.1	14	Inverted V-shape
[24]	32×32	$0.17\lambda_o^2$	4.14/6.1/8.32	30.8/31.4/34.2	4.26/4.41/6.27	15/16/20	Modified I-shape
[18]	-	-	6.77/8.57/13.37	15.6/23/17	4.67/5.15/5.8	14	Dumbbell shape
This work	29×29	$0.25\lambda_o^2$	5.23/7.50/10.82	43.27/47.84/45.17	7.33/6.66/6.28	25.46/28.17/32.59	NLR hexagonal patch with two rectangular narrow slots

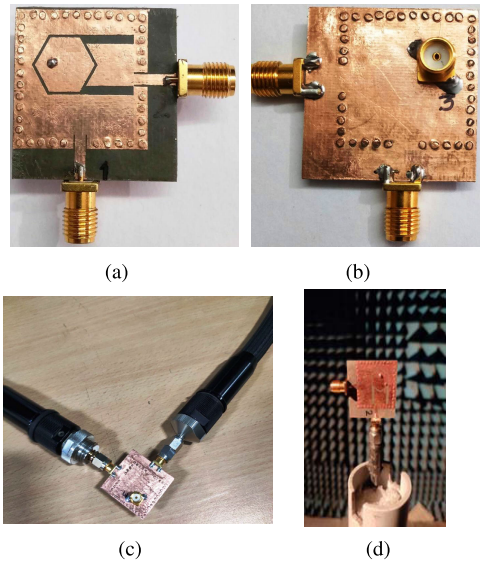

FIGURE 9. Fabricated prototype of the proposed STA (a) front side, (b) back side, (c) testing during VNA and (d) inside anechoic chamber for gain/efficiency and radiation pattern measurement.

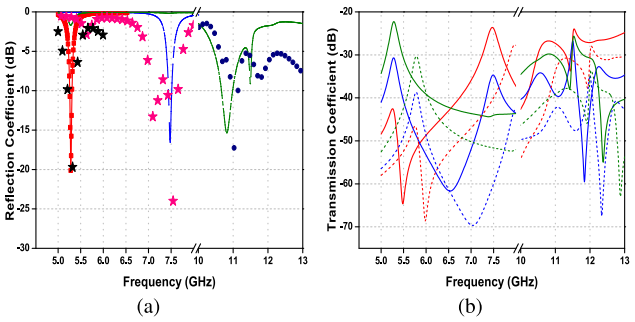

FIGURE 10. Comparison of simulated (solid line) and measured (dashed line) (a) reflection coefficient and (b) S_{21} (red), S_{31} (blue), S_{32} (green).

The gain and far-field measurement are performed inside the anechoic chamber with measurement setup as shown in

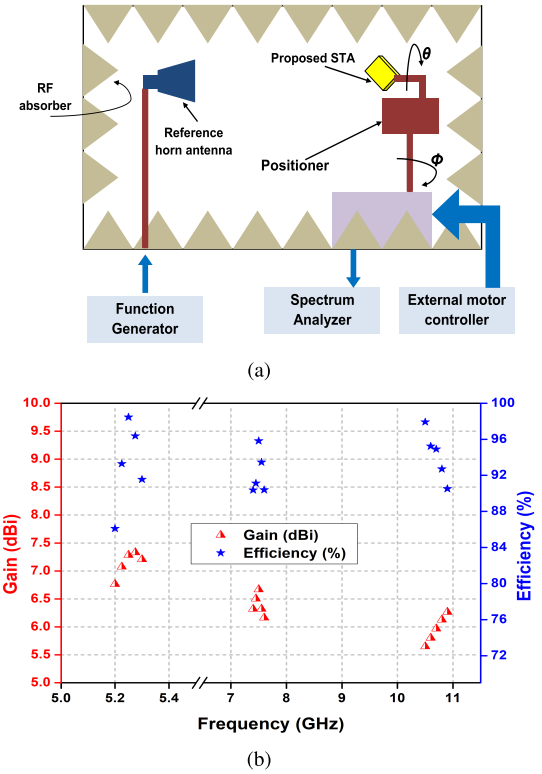

FIGURE 11. (a) Gain and radiation pattern measurement set-up sketch and (b) measured gain/efficiency of the triplexing antenna.

Fig. 11(a). The measured (simulated) peak gain values are 7.33 (7.65) dBi, 6.66 (6.93) dBi, and 6.28 (6.74) dBi at lower band, middle band, and upper frequency bands, respectively as reported in Fig. 11(b). It is noted that gain within a particular frequency band is obtained by applying excitation at only one port while terminated other two ports with matched 50Ω. The slight variations between simulated and measured values can be attributed to the soldering joints, uncontrolled dielectric losses, and fabrication imperfections.

TABLE 3. Simulated and (measured) results of proposed STA.

Parameters \ Excitation	Excitation Port		
	Port-1	Port-2	Port-3
Resonating frequency (GHz)	5.33 (5.28)	7.53 (7.48)	11.02 (10.81)
10 dB bandwidth (MHz)	50 (47)	71 (69)	310 (304)
Isolation (dB)	>40	>40	>40
Gain (dBi)	7.33 (7.65)	6.66 (6.93)	6.28 (6.74)
FTBR (dB)	25.46	28.17	32.59
Efficiency (%)	97.39	95.82	97.83

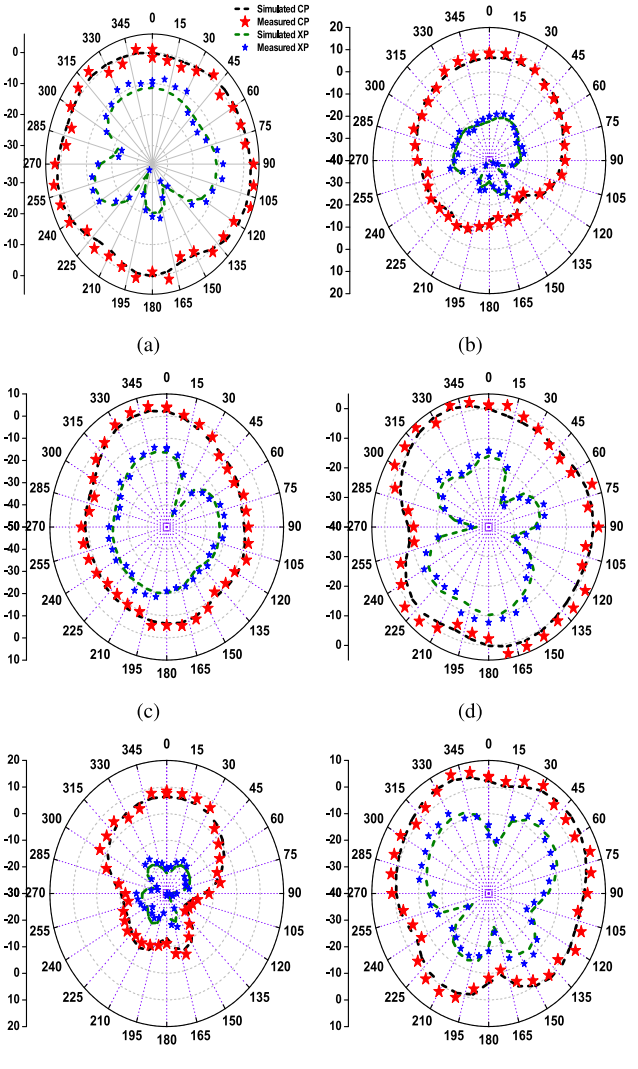

FIGURE 12. Simulated (solid line) and measured (dotted line) radiation patterns of the proposed STA. *E*-plane at (a) 5.33 GHz, (b) 7.53 GHz and (c) 11.02 GHz and *H*-plane at (d) 5.23 GHz, (e) 7.53 GHz and (f) 11.02 GHz.

The simulated and measured radiation patterns for three operating frequency bands (5.33, 7.53 and 11.02 GHz) in two orthogonal planes (ϕ=0° and ϕ=90°) are compared in Fig. 12. In both ϕ=0° and ϕ=90° planes, the co-polarization to cross-polarization difference for all resonating frequencies is ≥16.5 dB. It is seen that the measured responses are consistent with the simulated ones for the proposed STA. A little deviation between the two is observed which is probably due to the fixing of SMA connector and fabrication tolerances. In the similar manner, the FTBR reported in all three bands is better than 25 dB. This makes the proposed STA a suitable candidate for applications that falls within the below frequency ranges, as listed in Table 1.

The advantages of the proposed STA highlighted in Table 2. Here, a detailed comparative study with the already proposed STAs in the literature in terms of physical/electrical size, isolation, gain, efficiency, FTBR and complexity is summarized. The proposed STA possesses compact size along with high isolation among the ports and good gain/efficiency levels than the existing literature.

IV. CONCLUSION

A compact SIW cavity backed antenna with enhanced self-triplexing property is presented. The designed antenna supports operation in three different frequency bands, i.e., 5.23, 7.50 and 10.82 GHz simultaneously. The proposed design comprised of single SIW cavity loaded with hexagonal slot merged with two rectangular narrow slots. Initially, the fundamental TE_{110} mode along with two degenerated TE_{120} and TE_{210} modes are excited inside the SIW cavity with the help of orthogonally placed microstrip feed lines. Due to slot loading, the fundamental mode along with degenerate modes shift towards lower frequency, leading to overall size compactness of 68% as compared to [19]. Up to this stage, the proposed design supports two frequency bands centered around 5.23 and 7.50 GHz. For self-triplexing operation, a parasitic patch (similar to hexagonal slot) is placed concentrically inside it. This enabled the antenna to work in 10.82 GHz frequency band as well. The proposed self-triplexing antenna allows independent tuning of all three frequency bands using a single parameter/variable. High isolation among the excitation ports (>40 dB), good gain level (>6 dBi), high FTBR (>25 dB), and compact size ($0.25\lambda_o^2$) make the proposed triplexer a preferable candidate for both C- and X-band applications including WLAN/5G/WiMAX/Wi-Fi, amateur radio and satellite operations.

REFERENCES

[1] M. Kumar and V. Nath, "Introducing multiband and wideband microstrip patch antennas using fractal geometries: Development in last decade," *Wireless Pers. Commun.*, vol. 98, no. 2, pp. 2079–2105, Jan. 2018, doi: 10.1007/s11277-017-4965-x.

[2] S. C. Chen, Y. S. Wang, and S. J. Chung, "A decoupling technique for increasing the port isolation between two strongly coupled antennas," *IEEE Trans. Antennas Propag.*, vol. 56, no. 12, pp. 3650–3658, Dec. 2008, doi: 10.1109/TAP.2008.2005469.

[3] X. Meng, B. Chi, Y. Liu, T. Ma, and Z. Wang, "A fully integrated 150-GHz transceiver front-end in 65-nm CMOS," *IEEE Trans. Circuits Syst. II, Exp. Briefs*, vol. 66, no. 4, pp. 602–606, Apr. 2019, doi: 10.1109/TCSII.2018.2870926.

[4] M. Karlsson and S. Gong, "A frequency-triplexed inverted-F antenna system for ultra-wide multi-band systems 3.1–4.8 GHz," *ISAST Trans. Electron. Signal Process.*, vol. 1, no. 1, pp. 95–100, 2007.

[5] P. Cheong, K.-F. Chang, W.-W. Choi, and K.-W. Tam, "A highly integrated antenna-triplexer with simultaneous three-port isolations based on multi-mode excitation," *IEEE Trans. Antennas Propag.*, vol. 63, no. 1, pp. 363–368, Jan. 2015, doi: 10.1109/TAP.2014.2364299.

[6] D.-K. Park, R. Waterhouse, Y. Qian, and T. Itoh, "Self-diplexed integrated antenna transceiver for wireless applications," in *IEEE Antennas Propag. Soc. Int. Symp. Dig. Held Conjunct USNC/URSI Nat. Radio Sci. Meeting*, vol. 3, Jul. 2001, pp. 444–447, doi: 10.1109/APS.2001.960130.

[7] Y. Chung, S.-S. Jeon, D. Ahn, J.-I. Choi, and T. Itoh, "High isolation dual-polarized patch antenna using integrated defected ground structure," *IEEE Microw. Wireless Compon. Lett.*, vol. 14, no. 1, pp. 4–6, Jan. 2004, doi: 10.1109/LMWC.2003.821501.

[8] F. J. Herraiz-Martinez, E. Ugarte-Munoz, V. Gonzalez-Posadas, L. E. Garcia-Munoz, and D. Segovia-Vargas, "Self-diplexed patch antennas based on metamaterials for active RFID systems," *IEEE Trans. Microw. Theory Techn.*, vol. 57, no. 5, pp. 1330–1340, May 2009, doi: 10.1109/TMTT.2009.2017301.

[9] L. Inclan-Sanchez, J. L. Vaquez-Roy, and E. Rajo-Iglesias, "High isolation proximity coupled multilayer patch antenna for dual-frequency operation," *IEEE Trans. Antennas Propag.*, vol. 56, no. 4, pp. 1180–1183, Apr. 2008, doi: 10.1109/TAP.2008.919218.

[10] J. Montero-de-Paz, E. Ugarte-Muñoz, F. J. Herraiz-Martinez, V. González-Posadas, L. E. García-Muñoz, and D. Segovia-Vargas, "Multifrequency self-diplexed single patch antennas loaded with split ring resonators," *Prog. Electromagn. Res.*, vol. 113, pp. 47–66, 2011, doi: 10.2528/PIER10121703.

[11] S. Fallahzadeh, H. Bahrami, A. Akbarzadeh, and M. Tayarani, "High-isolation dual-frequency operation patch antenna using spiral defected microstrip structure," *IEEE Antennas Wireless Propag. Lett.*, vol. 9, pp. 122–124, 2010, doi: 10.1109/LAWP.2010.2043810.

[12] Y. Rikuta and H. Arai, "A self-diplexing antenna using stacked patch antennas," in *IEEE Antennas Propag. Soc. Int. Symp. Transmitting Waves Prog. Next Millennium Dig. Held Conjunct USNC/URSI Nat. Radio Sci. Meeting C*, vol. 4, Jul. 2000, pp. 2212–2215, doi: 10.1109/APS.2000.874933.

[13] L. Inclan-Sanchez, J.-L. Vazquez-Roy, and E. Rajo-Iglesias, "Diplexed dual-polarization proximity coupled patch antenna," in *Proc. IEEE Antennas Propag. Soc. Int. Symp.*, Jun. 2007, pp. 2061–2064, doi: 10.1109/APS.2007.4395930.

[14] M. Bozzi, L. Perregrini, K. Wu, and P. Arcioni, "Current and future research trends in substrate integrated waveguide technology," *Radioengineering*, vol. 18, no. 2, pp. 201–209, 2009.

[15] A. Kumar, M. Kumar, and A. K. Singh, "Substrate integrated waveguide cavity backed wideband slot antenna for 5G applications," *Radioengineering*, vol. 30, no. 3, pp. 480–487, Sep. 2021, doi: 10.13164/re.2021.0480.

[16] N. Nguyen-Trong and C. Fumeaux, "Half-mode substrate-integrated waveguides and their applications for antenna technology: A review of the possibilities for antenna design," *IEEE Antennas Propag. Mag.*, vol. 60, no. 6, pp. 20–31, Dec. 2018, doi: 10.1109/MAP.2018.2870587.

[17] K. Kumar and S. Dwari, "Substrate integrated waveguide cavity-backed self-triplexing slot antenna," *IEEE Antennas Wireless Propag. Lett.*, vol. 16, pp. 3249–3252, 2017, doi: 10.1109/LAWP.2017.2771510.

[18] S. Mukherjee, S. Ghosh, and A. Biswas, "Design of compact SIW cavity backed self-triplexing planar slot antenna for triple band application," in *Proc. 15th Eur. Conf. Antennas Propag. (EuCAP)*, Mar. 2021, pp. 1–5, doi: 10.23919/EuCAP51087.2021.9411029.

[19] D. Chaturvedi, A. Kumar, and S. Raghavan, "An integrated SIW cavity-backed slot antenna-triplexer," *IEEE Antennas Wireless Propag. Lett.*, vol. 17, no. 8, pp. 1557–1560, Aug. 2018, doi: 10.1109/LAWP.2018.2855051.

[20] A. Iqbal, M. A. Selmi, L. F. Abdulrazak, O. A. Saraereh, N. K. Mallat, and A. Smida, "A compact substrate integrated waveguide cavity-backed self-triplexing antenna," *IEEE Trans. Circuits Syst. II, Exp. Briefs*, vol. 67, no. 11, pp. 2362–2366, Nov. 2020, doi: 10.1109/TCSII.2020.2966527.

[21] A. Kumar and S. Raghavan, "Design of SIW cavity-backed self-triplexing antenna," *Electron. Lett.*, vol. 54, no. 10, pp. 611–612, May 2018, doi: 10.1049/el.2017.4775.

[22] A. Kumar, D. Chaturvedi, M. Saravanakumar, and S. Raghavan, "SIW cavity-backed self-triplexing antenna with T-shaped slot," in *Proc. Asia–Pacific Microw. Conf. (APMC)*, Nov. 2018, pp. 1588–1590, doi: 10.23919/APMC.2018.8617526.

[23] S. Priya and S. Dwari, "A compact self-triplexing antenna using HMSIW cavity," *IEEE Antennas Wireless Propag. Lett.*, vol. 19, no. 5, pp. 861–865, May 2020, doi: 10.1109/LAWP.2020.2982533.

[24] S. K. K. Dash, Q. S. Cheng, R. K. Barik, N. C. Pradhan, and K. S. Subramanian, "A compact triple-fed high-isolation SIW-based self-triplexing antenna," *IEEE Antennas Wireless Propag. Lett.*, vol. 19, no. 5, pp. 766–770, May 2020, doi: 10.1109/LAWP.2020.2979488.

[25] F. Xu and K. Wu, "Guided-wave and leakage characteristics of substrate integrated waveguide," *IEEE Trans. Microw. Theory Techn.*, vol. 53, no. 1, pp. 66–73, Jan. 2005, doi: 10.1109/TMTT.2004.839303.

[26] G. Q. Luo, Z. F. Hu, Y. Liang, L. Y. Yu, and L. L. Sun, "Development of low profile cavity backed crossed slot antennas for planar integration," *IEEE Trans. Antennas Propag.*, vol. 57, no. 10, pp. 2972–2979, Oct. 2009, doi: 10.1109/TAP.2009.2028602.

[27] U. Schmiade, "Antenna and method of design," U.S. Patent 2004 0 017 317 A1, Jan. 29, 2004.

[28] A. Chand, M. Kumar, and V. Nath, "Triple band non-linear manipulated Sierpinski–Knopp fractal wide-slot microstrip antenna with inverted L-shaped strip," in *Proc. 2nd Int. Conf. Electron., Mater. Eng. Nano-Technol. (IEMENTech)*, May 2018, pp. 1–7, doi: 10.1109/IEMENTECH.2018.8465193.

[29] M. Kumar and V. Nath, "Microstrip-line-fed elliptical wide-slot antenna with similar parasitic patch for multiband applications," *IET Microw., Antennas Propag.*, vol. 12, no. 14, pp. 2172–2178, Nov. 2018, doi: 10.1049/iet-map.2018.5377.

AMIT KUMAR was born in Agra, Uttar Pradesh, India, in 1993. He received the B.Tech. degree in electronics and communication engineering from the Ambedkar Institute of Advanced Communication Technologies and Research, affiliated to Guru Gobind Singh Indraprastha University (GGSIPU), India, in 2014, and the master's degree in electronics and communication (ECE) from the University School of Information, Communication and Technology (USIC&T), GGSIPU, in 2016. He is currently pursuing the Ph.D. degree with IIT (BHU), Varanasi, India. His research interests include SIW-based antennas and circuits, broadband antennas, circularly polarized antennas MMW, and THz bands.

MUNISH KUMAR (Graduate Student Member, IEEE) was born in New Delhi, India, in 1990. He received the M.Tech. degree in ECE from USIC&T, GGSIPU, New Delhi, in 2015, where he is currently pursuing the Ph.D. degree. He has worked extensively and authored more than 20 research articles on multiband and wideband microstrip patch antennas, fractals, electromagnetic bandgap structures (EBG), circularly polarized, and MIMO antennas in various international journals and conferences. His current research interests include designing of microstrip antennas for wideband and multiband applications.

AMIT KUMAR SINGH received the Ph.D. degree from IIT (BHU), Varanasi, in 2010. He has been working as an Associate Professor with the Electronics Engineering Department, IIT (BHU), since 2012. He has published and coauthored over 70 journal articles and conference papers. His research interests include the areas of design of millimeter frequency antennas, feeds for parabolic reflectors, dielectric resonator antennas, microstrip antennas, EBG, artificial magnetic conductors, soft and hard surfaces, antennas for RFIDs, phased array antennas, and computer aided design for antennas.